ACS APPLIED MATERIALS & INTERFACES

Research Article

www.acsami.org

Supported Planar Mammalian Membranes as Models of in Vivo Cell Surface Architectures

Han-Yuan Liu,[†] Hannah Grant,[†] Hung-Lun Hsu,[†] Raya Sorkin,[‡] Filip Bošković,[‡] Gijs Wuite,[‡] and Susan Daniel*[,†]

[†]School of Chemical and Biomolecular Engineering, Cornell University, Ithaca, New York 14853, United States

[‡]Department of Physics and Astronomy and Laser Lab, Vrije Universiteit Amsterdam, Amsterdam 1081 HV, The Netherlands

ABSTRACT: Emerging technologies use cell plasma membrane vesicles or "blebs" as an intermediate to form molecularly complete, planar cell surface mimetics that are compatible with a variety of characterization tools and microscopy methods. This approach enables direct incorporation of membrane proteins into supported lipid bilayers without using detergents and reconstitution and preserves native lipids and membrane species. Such a system can be advantageous as in vitro models of in vivo cell surfaces for study of the roles of membrane proteins as drug targets in drug delivery, host−pathogen interactions, tissue engineering, and many other bioanalytical and sensing applications. However, the impact of methods used to induce cell blebbing (vesiculation) on protein and membrane properties is still unknown. This study focuses on characterization of cell blebs created under various bleb-inducing conditions and the result on protein properties (orientation, mobility, activity, etc.) and lipid scrambling in this platform. The orientation of proteins in the cell blebs and planar bilayers is revealed using a protease cleavage assay. Lipid scrambling in both cell blebs and planar bilayers is indicated through an annexin V binding assay. To quantify protein confinement, immobility, etc., incorporation of GPI-linked yellow fluorescent protein (GPI-YFP) was used in conjunction with single-molecule tracking (SMT) microscopy. Finally, to investigate the impact of the bleb induction method on protein activity and expression level, cell blebs expressing human aminopeptidase N (hAPN) were analyzed by an enzyme activity assay and immunoblotting. This work enriches our understanding of cell plasma membrane bleb bilayers as a biomimetic platform, reveals conditions under which specific properties are met, and represents one of the few ways to make molecularly complete supported bilayers directly from cell plasma membranes.

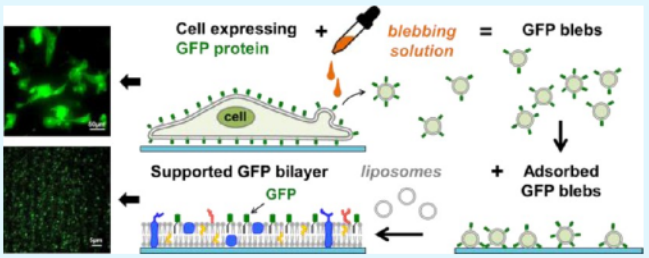

KEYWORDS: *Supported lipid bilayer, cell plasma membrane vesicles, planar mammalian cell membrane, single-molecule tracking, protein diffusion, cell blebs*

1. INTRODUCTION

Biological membranes comprised of phospholipids and proteins are a specialized permeability barrier encapsulating the cell cytosol and organelles and are important for regulating the interaction between cells and their external environment. Proteins in biological membranes have critical roles in molecular-scale processes necessary for cell function, such as material transport, signaling, and recognition.[1−4] Furthermore, interactions of lipids with proteins are crucial for regulating protein activity in these various roles.[5,6] In order to understand how lipid−protein interactions regulate membrane protein function in biological membranes, cell-based assays are often used. The advantage of cell-based assay is the ability to preserve the native environment. However, the complexity and dynamism of cells makes such assays inconvenient for isolating the effect of individual factors on the studies at hand. On the other hand, the traditional characterization techniques for lipid−protein interaction using detergents to extract membrane proteins changes the structure and function of proteins and may artificially change the native lipid−protein association.[5,7,8] Thus, alternative membrane platforms that bridge in vivo and in vitro environments and are compatible with a wide variety of characterization techniques can greatly assist in understanding how membrane proteins function and are regulated. Such platforms can also be employed in a variety of bioanalytical and sensing applications, which leverage the relationship between protein and lipid on biological function.

A supported lipid bilayer (SLB) can be formed on a solid surface using vesicle rupture,[9] the solvent-assisted lipid bilayer formation method,[10] or Langmuir−Blodgett−Schaeffer transfer techniques.[11] Because of its planar geometry, the SLB is compatible with various surface characterization tools such as total internal reflection fluorescence (TIRF) microscopy,[12] atomic force microscopy (AFM),[13] quartz crystal microbalance,[14] and surface plasmon resonance.[15] However, the challenges of incorporating membrane proteins into SLBs are significant, namely, with regard to their orientation, fluidity, and function. In our previous work[16−18] we demonstrated that

Received: May 26, 2017
Accepted: September 20, 2017
Published: September 20, 2017

DOI: 10.1021/acsami.7b07500
ACS Appl. Mater. Interfaces XXXX, XXX, XXX−XXX

membrane proteins can be introduced into SLBs using cell plasma membrane "blebs" without using detergents or vesicle reconstitution (Figure 1A). Cell plasma membrane blebs are

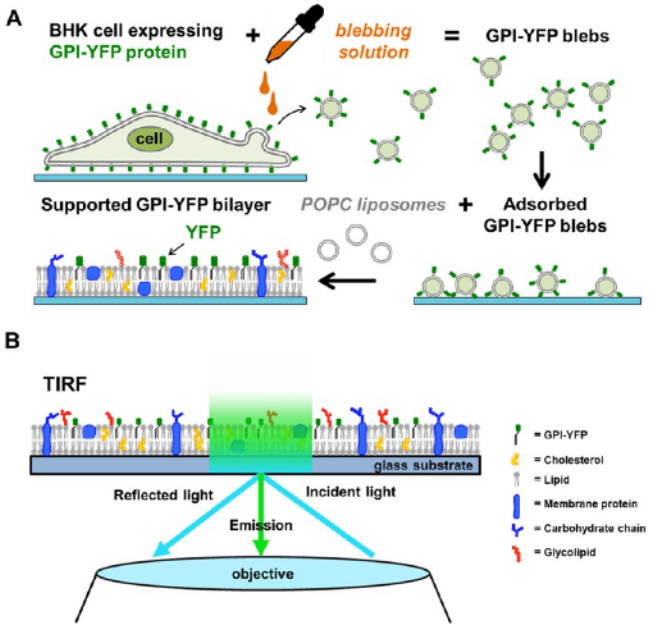

Figure 1. (A) BHK cells expressing GPI-YFP were induced to generate cell plasma membrane blebs, which were subsequently adsorbed and ruptured to form a cell plasma membrane bleb bilayer. (B) TIRF microscopy was used to investigate the protein mobility and activity in cell plasma membrane bleb bilayers.

proteoliposomes that bud from the cell surface, induced by either chemical reagents or serum starving. These proteoliposomes retain the lipid and protein diversity of the cellular membrane. Although cell blebbing allows the incorporation of membrane protein into SLBs without the need for detergents and reconstitution, there are key aspects that need to be investigated regarding the impact of the means by which blebs are produced (chemical versus chemical free) on protein and lipid properties, namely, protein orientation, mobility, level, activity, and membrane leaflet asymmetry.

Formaldehyde (FA) and dithiothreitol (DTT) are commonly used in the chemical blebbing process. FA is known to be a protein cross-linking agent when applied to cells at higher concentrations (4%).[19,20] DTT reduces disulfide bonds and palmitoylated cysteines, which can impact lipid phase partitioning.[20−22] To investigate the impact of chemical and chemical-free (serum-starving) means on producing cell membrane blebs and cell membrane bleb bilayers, we varied the concentration of FA/DTT in blebbing solutions or employed serum starving to induce baby hamster kidney (BHK) cells to vesiculate, or "bleb".[23] The resulting blebs were characterized for size, concentration, zeta potential, and resilience. Blebs and planar bilayers formed from them were characterized for protein content and protein and lipid orientation. Protein mobility, confinement, and activity were assessed in planar bilayers.

Glycophosphatidylinositol proteins (with lipid anchor) are located on the extracellular leaflet of the plasma membrane and are involved in a variety of biological process such as signaling, catalysis, enzymatic, and cell adhesion.[24,25] Using TIRF microscopy, planar bilayers formed from cell plasma membrane blebs expressing glycophosphatidylinositol-anchored yellow fluorescent protein (GPI-YFP) is a simple way to study protein mobility via single-molecule tracking (SMT) (Figure 1B). With SMT, single fluorescent proteins are tracked and analyzed to determine the protein mobility, diffusivity, and confinement trends under various blebbing conditions. To assess protein orientation, a protease cleavage assay was used to indicate the orientation of GPI-YFP. To assess lipid asymmetry, phosphatidylserine (PS) lipid orientation in cell plasma membrane blebs and cell plasma membrane bleb bilayer was revealed through an annexin V binding assay. To assess protein activity under various blebbing conditions, human aminopeptidase N (hAPN), a membrane-bound enzyme, was subjected to an enzyme activity assay. hAPN plays multiple roles in physiological processes including metabolism, cell motility and adhesion, and coronavirus binding and entry.[26−28] hAPN expression levels under these different blebbing conditions was revealed via immunoblotting.

From our analysis of these experiments, we find that cell membrane bleb bilayers used as a biomimetic mammalian cell surface platform preserve protein orientation, mobility, and activity under certain conditions. We also discovered that blebs produced by chemical means are considerably different from serum-starvation-induced blebs. One drawback we discovered is that PS lipid asymmetry is not maintained in either blebbing process. Nonetheless, this platform is still a powerful tool for in vitro applications, having identified conditions where protein properties are best maintained. By combining planar cell membrane bleb bilayers with appropriate surface characterization techniques, these materials have been shown to be convenient platforms to quantitatively measure virus binding and entry.[17,18] With the complete characterization presented here, such a molecularly complete, planar-supported cell membrane, with maximally functional proteins, could be useful for myriad technological purposes from tissue engineering, to drug delivery screening, to advanced studies of virus binding and entry.

2. MATERIALS AND METHODS

2.1. Cells and Plasmids. Baby hamster kidney (BHK) cells are extensively used as successful host for stable expression of various recombinant proteins, substrates for virus propagation for vaccines, and a crucial member of mammalian expression systems for pharmaceutical production.[29−31] BHK cells used in our work were obtained from the American Type Culture Collection (ATCC) and grown in Dulbecco's modified Eagle medium (DMEM) (CellGro) supplemented with 10% fetal bovine serum (Gibco), 100 U/mL penicillin and 10 μg/mL streptomycin (CellGro), and 1% HEPES buffer (CellGro). The pYFP-GPI-N1 plasmid was obtained from the Baird/Holowka research group at Cornell University and used for transfection of BHK cells to express a glycophosphatidylinositol (GPI) anchored yellow fluorescent (YFP) protein. The pCI-neo-hAPN plasmid was the generous gift from Kathryn Holmes of the University of Colorado and used for transfection of BHK cells to express the human aminopeptidase N (hAPN).

2.2. Preparation of Liposomes. The following lipids were used in these experiments: 1-oleoyl-2-palmitoyl-*sn*-glycero-3-phosphocholine (POPC) and 1-palmitoyl-2-oleoyl-*sn*-glycero-3-phospho-L-serine (POPS), purchased from Avanti Polar Lipids. The liposomes were prepared by mixing the components in chloroform (Sigma) in the desired ratio. Chloroform was gently evaporated using a stream of nitrogen; then the lipid films were stored under vacuum for 3 h to remove any residual chloroform. To create liposomes, phosphate-buffered saline (PBS) buffer (5 mM NaH_2PO_4, 5 mM Na_2HPO_4, 150 mM NaCl at pH 7.4) was added to the dried films to a concentration

DOI: 10.1021/acsami.7b07500
ACS Appl. Mater. Interfaces XXXX, XXX, XXX−XXX

of 2 mg/mL. Single unilamellar liposomes were prepared by extrusion using a 50 nm membrane (Nucleopore Polycarbonate, GE Health) with at least 15 passes. Two formulations were used in this study: The first is pure POPC, and the second contains 98% POPC and 2% POPS. The first preparation, POPC liposomes, is used in forming the supported planar bilayer with the cell plasma membrane blebs. The second formulation, 98% POPC/2% POPS liposomes, is used to form the supported lipid bilayer containing PS to verify the binding of Annexin V-FITC (Molecular Probes) as a control.

2.3. Preparation of Plasma Cell Membrane Blebs. There were 9×10^6 cells/mL BHK cells seeded in 10 cm Petri dishes (Corning) and incubated for 24 h in a 37 °C, 5% CO_2 incubator. Transfection was performed by using 18 μL of Turbofect transfection reagent (ThermoScientific) and 6 μg of DNA plasmid, pYFP-GPI-N1, and incubated for 24 h in a 37 °C, 5% CO_2 incubator. After 24 h, the cells were washed with GPMV buffer (2 mM $CaCl_2$, 10 mM HEPES, 150 mM NaCl at pH 7.4) and then blebbing buffer, which is 4 mL of GPMV buffer with various amounts of formaldehyde (FA) and dithiothreitol (DTT) to induce cell bleb budding. For example, for our solution denoted as "0.075% FA", it consists of 25 mM formaldehyde (FA) and 2 mM dithiothreitol (DTT). Various concentrations of blebbing solutions denoted as 0.01%, 0.075%, 1.5%, 3.0%, and 4.0% FA (with the corresponding ratioed DTT concentrations) were used in these studies. The cells were incubated in the blebbing solution for 1 h at 37 °C. The other method used here to induce cell blebbing is serum starving (SS).[23] Here cells were washed by 6 mL of Dulbecco's modified Eagle medium and 4 mL of Dulbecco's modified Eagle medium without fetal bovine serum. This mixture was added into the plates to induce the cell blebbing. In both cases, after incubation for 1 h at 37 °C, the buffer was removed from the culture and the cell blebs within it were settled on ice for 15 min to separate cell debris and cell blebs. Only the upper 75% of the volume of settled, iced solution was used in subsequent experiments.

2.4. AFM Characterization of Bleb Resilience and Morphology. Imaging of blebs was conducted on piranha-cleaned glass surfaces. Imaging of bilayer by AFM was conducted on poly L-lysine surfaces. For force spectroscopy, blebs were attached to piranha-cleaned glass-coated glass slides in their corresponding buffer. Slides were first cleaned in a 96% ethanol, 3% HCl solution for 10 min. Next, they were coated for 1 h in a 0.001% poly-L-lysine (Sigma) solution, rinsed with ultrapure water, and dried overnight at 37 °C. Coated slides were stored at 7 °C for a maximum of 1 month. Blebs were imaged in PeakForce Tapping mode on a Bruker Bioscope catalyst setup. The force set point during imaging was 100−200 pN. Nanoindentations were performed by first making an image of a single particle and then indenting it until a trigger force of 10 nN is reached at a velocity of 250 nm/s. Prior to performing each nanoindentation, the tip was checked for adherent lipid bilayers by obtaining a force curve on a glass surface until a trigger force of 5 nN was obtained. Tips used were either silicon nitride tips with a nominal tip radius of 15 nm on a 0.1 N/m cantilever by Olympus (OMCL-RC800PSA) or Bruker SNL silicon nitride tips on a 0.12 N/m cantilever with a nominal tip radius of 2 nm. All presented force spectroscopy data was obtained using Bruker SNL cantilevers. Individual cantilevers were calibrated using thermal tuning. Data analysis of nanoindentation curves was done using Gwyddion software. Image processing of flattened images was carried out using the freely available software WSXM.[32]

2.5. Characterization of Bleb Size, Zeta Potential, and Concentration. Nanoparticle tracking analysis (NTA, Nanosight NS300, Malvern) was used to determine the size and concentration of blebs in the supernatant. Laser doppler electrophoresis (Zetasizer Nano ZS, Malvern) was used to measure the zeta potential of blebs. For measurement of zeta potential, serum-starved blebs were measured in Dulbecco's modified Eagle medium and chemically induced blebs were measured in GPMV buffer, as described above.

2.6. Scanning Electron Microscopy (SEM). To confirm our NTA data and check the morphology of the vesicles, cryo-SEM was employed to image the blebs. A small drop of the bleb solution (0.075% FA sample) was placed onto a carbon film TEM grid. A second grid was then gently placed on top of the drop and gently pulled over the first grid, spreading the sample into a thin film on both grids. The prepared grids, mounted on a transfer shuttle, were plunge-frozen in liquid nitrogen. They were then loaded under vacuum onto the stage (−165 °C) in a cryo-preparation chamber (Quorum model PP3010). In the chamber, the ice sublimed at −100 °C for 60 s. Following this step, the sample was loaded onto the cryo stage (−165 °C) inside the scanning electron microscope (SEM) equipped with a focused ion beam (FIB) system (Thermo Fisher (formerly FEI) Strata 400S) for imaging.

2.7. Preparation for Planar Bleb Bilayer Formation. Polydimethylsiloxane (PDMS) wells were made with a 10:1 elastomer/cross-linker mixture of Sylgard 184 (Robert McKeown Co.) and baked for 5 h at 78 °C. PDMS wells were attached to dry, clean glass slides (25 × 25 mm No. 1.5, VWR). The glass slides were pretreated by piranha solution (70% (v/v) H_2SO_4 (BDH) and 30% (v/v) H_2O_2 (Sigma 50 wt %)) for 10 min and rinsed by flushing DI water for 20 min continuously. Next, 100 μL of solution containing blebs at approximately 5×10^8 blebs/mL was added into the well and incubated for 15 min. After incubation, the well was rinsed gently with PBS buffer to remove the unattached blebs. A 100 μL amount of liposomes at 2 mg/mL was added into the well and incubated for 30 min to form the bleb bilayer. After the bleb bilayer formed, the well was rinsed with PBS buffer again to remove the excess unruptured liposomes.

2.8. Protease Cleavage Assay for Protein Orientation in Cell Blebs and Planar Bleb Bilayers. Proteinase K (Sigma) in the form of lyophilized powder was added to a storage buffer (20 mM Tris-HCl, 1 mM $CaCl_2$, 50% glycerol at pH 7.4) at 20 mg/mL and stored at −20 °C. The proteinase K solution was diluted to 100 μg/mL with Tris-HCl buffer (20 mM Tris-HCl at pH 7.4) to conduct the protease cleavage assay. For determination of GPI-YFP orientation in either the blebs or the bleb bilayer, 100 μL of 100 μg/mL proteinase K was added to either blebs or bleb bilayer on glass slides at various blebbing conditions. Images were recorded using TIRF microscopy at 15 min intervals to track proteinase K cleavage, which is registered when the fluorescent domain of protein leaves the evanescent field, resulting in the loss of fluorescent signals in blebs and bleb bilayer. This signal loss was quantified by particle counting. The number of fluorescent particles was compared to control samples without adding proteinase K. The results are used to infer the orientation of GPI-YFP in the blebs and bleb bilayer.

2.9. Annexin V Assay for Lipid Orientation in Cells, Cell Blebs, and Planar Bleb Bilayers. Annexin V conjugated with FITC is a protein that preferentially binds phosphatidylserine (PS) and is strongly calcium dependent. PS is commonly found on the internal leaflet of cell plasma membrane of live cells. Early in the process of apoptosis the asymmetry of the membrane is disrupted such that PS becomes exposed on the external leaflet of cell plasma membrane.[33]

Cells. BHK cells expressing hAPN were rinsed with binding buffer (10 mM Tris, 100 mM NaCl, and 8 mM $CaCl_2$ at pH 7.4), and then 5 μL of annexin V was added to the culture and incubated for 30 min. After incubation, the cells were rinsed with PBS buffer. The images of BHK cells were recorded by an inverted Zeiss Axio Observer.Z1 microscope with α Plan-Apochromat 20× objective. For cells treated by serum starving or 0.075% FA, the assay was carried out in the same manner postblebbing.

Intact Cell Blebs. Blebs adsorbed on glass slides were rinsed with bovine serum albumin (BSA, Sigma) at 0.1 mg/mL for 30 min to block exposed glass to prevent false positives. Wells were then rinsed with binding buffer, and 2 μL of annexin V was added and incubated for 30 min. Then the wells were rinsed with PBS buffer to remove the excess unbound annexin V. Binding level was assessed with fluorescence microscopy.

Planar Bilayers. For the control cases, 100 μL of POPC liposomes or 98% POPC/2% POPS liposomes at 2 mg/mL were added respectively to wells and incubated for 30 min to form bilayers. After SLB formation, the wells were rinsed with binding buffer and 2 μL of annexin V was added and incubated for 30 min. Finally, the wells were rinsed with PBS buffer to remove the excess unbound annexin V.

DOI: 10.1021/acsami.7b07500
ACS Appl. Mater. Interfaces XXXX, XXX, XXX−XXX

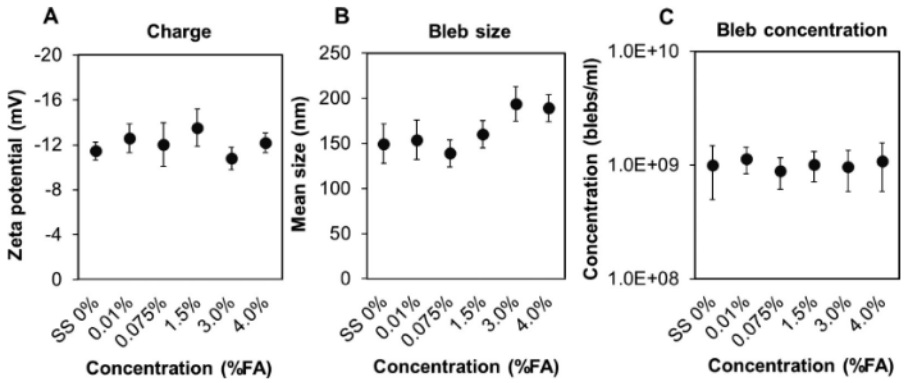

Figure 2. Characterization of bleb zeta potential, size, and concentration. Blebs are produced by various FA/DTT conditions indicated in the *x* axes. (A) Zeta potentials of blebs are relatively consistent around −12 mV. (B) Average size of the cell blebs increases slightly with increasing concentration of FA/DTT in the blebbing solution. (C) Concentrations of cell blebs remain constant with increasing concentration of FA/DTT.

Binding level was assessed with fluorescence microscopy. For the bleb bilayers on glass slides, after bilayer formation, they were also rinsed with BSA at 0.01 mg/mL for 30 min as a nonspecific blocking step. Wells were rinsed with binding buffer and 2 μL of annexin V added and incubated for 30 min. The wells were rinsed with PBS buffer to remove the excess unbound annexin V and imaged using fluorescence microscopy.

2.10. Characterization of the Motion of Individual Membrane Proteins by Single-Molecule Tracking. Various methods for single-molecule tracking (SMT) have already been described in previous literature.[34−37] Bleb bilayers incorporating the fluorescent protein, GPI-YFP, were imaged and recorded by total internal reflection microscopy (TIRF). The settings and operation of the microscope are described below. To enable accurate tracking, all trajectories were found and calculated by using the single-molecule tracking method previously reported.[16] This method determines the particle locations by their intensity, change of intensity from previous frame, and displacement from previous frame to find the match for every trajectory.[38] A particle that only moves around inside an area smaller than the maximum observed displacement for immobile fluorescent beads in the system is regarded as immobile.[39] The SMT algorithm uses the initial slope of the mean squared displacement (MSD) from the first three time steps to determine the local "homogenous" diffusion coefficient.[40,41] Therefore, the heterogeneity of bleb bilayer or change of diffusion mode resulting from different domains does not strongly influence the initial diffusion coefficient for short times. To assess this heterogeneity, we employ moment scaling spectrum (MSS) analysis[37,39] to quantify the mobility of a particle via parameter β. Here, parameter β describes the type of motion for each particle: $\beta < 0.4$ is confined diffusion, $0.4 \leq \beta \leq 0.6$ is quasi-free diffusion, $\beta > 0.6$ is convective diffusion. All images were analyzed by using Matlab (Mathworks) and ImageJ (NIH).

2.11. Human Aminopeptidase N Enzyme (hAPN) Activity Assay. Human aminopeptidase N is widely expressed in many cell types and species and plays crucial roles in many biological processes such as cell adhesion, peptide metabolism, and virus binding. Human aminopeptidase N, a membrane-bound enzyme, cleaves the N-terminal amino acid from active proteins leading to its inactivation.[26−28] To analyze the impact of formaldehyde on the native enzymatic function of hAPN, an enzymatic activity assay was conducted to reveal the activity of hAPN in blebs from various blebbing conditions. H-Ala-AMC (Bachem) is the substrate for hAPN. As the hAPN cleaves the substrate, the substrate becomes fluorescent. Bleb concentration was controlled at 5×10^8 blebs/mL during these experiments. Mixtures of 500 μL of blebs and 500 μL of H-Ala-AMC at 270 mM in a 50 mM Tris buffer at pH 7.4 were added to a cuvette, and the fluorescent intensity was monitored for at least 1.5 h using a fluorometer (Photon Technologies International Inc.) at an excitation/emission of 380/460 nm.

2.12. Characterization of Protein Expression by Western Blot. After the blebbing process induced by either serum starving or FA/DTT exposure, cell bleb concentration was measured by NTA and normalized to the same value for all samples. In order to have enough material to conduct the immunostaining, samples were subsequently concentrated by ultracentrifuge in preparation for Western blotting. These cell bleb samples were centrifuged at 30 000 × g for 1 h, and the pellets were resuspended by GPMV buffer. The samples were mixed with 2 × Laemmli sample buffer (Bio-Rad) plus 10% DTT at a 1:1 ratio. The samples were incubated at 50 °C for 10 min. Then the samples were separated by SDS-PAGE (Bio-Rad) and transferred to a PVDF membrane (Millipore). The membrane was blocked with 5% dry fat milk in Tris-buffered saline plus 0.01% Tween-20 (TBST) at room temperature for 1 h and then incubated with 1:1000 anti-hAPN antibodies (Everest Biotech) at room temperature for 1 h. After washing with TBST, the membrane was rinsed in 1:2500 horseradish peroxidase conjugated-rabbit antigoat IgG antibodies (abcam). For the GPI-YFP case, the membrane was incubated with 1:2500 anti-GFP antibodies and then 1:2500 horseradish peroxidase conjugated-rabbit antimouse IgG antibodies. After washing with TBST, protein bands were visualized using an ECL detection system (Bio-Rad).

2.13. TIRF Microscope Settings and Operation. The GPI-YFP protein orientation, motion tracking, and annexin V binding for lipid orientation were conducted using total internal reflection fluorescence (TIRF) microscopy on an inverted Zeiss Axio Observer.Z1 microscope with an α Plan-Apochromat 100× objective. Wavelengths of 488 and 561 nm from solid-state lasers were used to excite the sample. A Laser TIRF 3 slider (Carl Zeiss, Inc.) was used to control angle of incidence at ~68°, generating the evanescent wave around 100 nm and total internal reflection. The excitation light was filtered by a Semrock LF488-B-ZHE filter cube and sent to the electron-multiplying CCD camera (ImageEM C9100-13, Hamamatsu).

3. RESULTS AND DISCUSSION

3.1. Characterization of Bleb Size, Zeta Potential, and Concentration. To investigate the impact of the chemicals used to induce blebbing on the properties of cell membrane blebs, six solutions covering a range of concentrations of chemicals were examined. These are denoted as 0.01%, 0.075%, 1.5%, 3%, and 4% formaldehyde (FA) with the appropriate amount of DTT to maintain the ratio of FA/DTT in GPMV buffer; DMEM was used for the serum-starving (SS) method (0% FA/DTT). The resulting blebs were examined using nanoparticle tracking analysis (NTA) and laser Doppler electrophoresis to assess their average size, zeta potential, and concentration. We found that the zeta potentials of blebs from various blebbing conditions were similar, at about −12 mV, which indicates that increasing FA/DTT concentration in blebbing solutions has a minimal effect on the zeta potential of blebs (Figure 2A). However, the size of blebs slightly increases

DOI: 10.1021/acsami.7b07500
ACS Appl. Mater. Interfaces XXXX, XXX, XXX−XXX

with the increasing concentration of FA/DTT (Figure 2B). The size range of cell blebs is between 100 and 500 nm with the average size of 150−200 nm. The concentrations of cell blebs isolated in the supernatant were consistently around 10^8−10^9 blebs/mL among all blebbing conditions (Figure 2C). Overall, the average size of the cell blebs increases about 50 nm with increasing concentration of FA/DTT used in the blebbing solution. However, increasing FA/DTT does not dramatically affect the concentration or the zeta potential of cell blebs over the range tested here, including the serum-starving case. It is important to note that as the size of cell blebs increases about 50 nm, the zeta potential, which is the surface charge density, does not change, but the total charge of the bleb will increase.

Cell plasma membrane blebs may contain a diverse size population of extracellular vesicles in solution, ranging over 100−500 nm, based on our measurements and previous literature.[42−44] Cell plasma membrane blebs may contain mainly two types of vesicles: one of smaller size, which derives from exocytosis, and the other of larger size that buds directly from cell plasma membrane. In Figure 2B, as the concentration of FA increases, the average size of cell blebs also increases. A possible explanation is that the chemically induced method may preferentially promote vesicle budding from cell plasma membrane, so the population of large vesicle increases. A comparison between the serum-starving (chemical-free) and the chemically induced method will be described and discussed in a later section.

3.2. Characterization of Bleb Morphology and Size Distribution by Cryo-SEM. Additional experiments were conducted to reveal the morphology of cell blebs, especially to confirm a hollowed-out structure of the vesicles, as depicted in Figure 1, and to confirm the size distributions reported by NTA. As shown in Figure 3, the SEM images indicate that the blebs are generally spherical in nature and that the size of cell blebs varies. However, the main size population of cell blebs is around 100−500 nm, matching the nanoparticle tracking analysis data reported above.

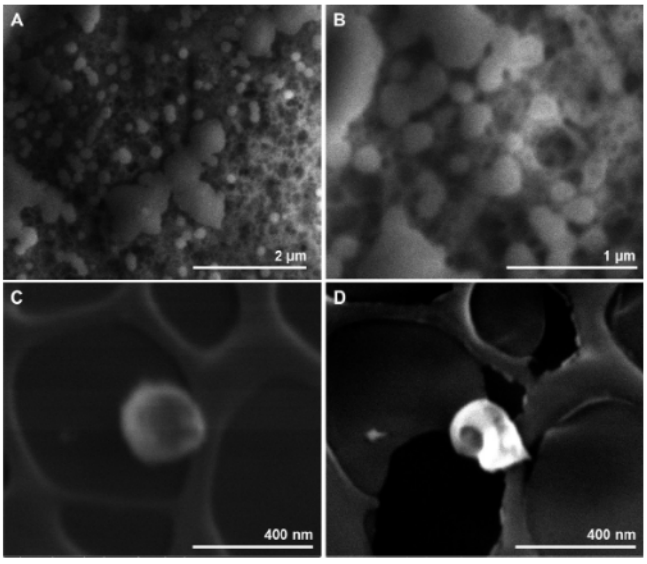

Figure 3. SEM images of cell blebs derived from 0.075% FA chemically induced method. (A) Top view image. (B) Top view image, more magnification. (C) Individual image is taken with the stage tilted at a 52° angle. (D) Same sample shown in C after focused ion beam treatment. Image is taken with the stage tilted at a 52° angle.

To gain some insight into the internal morphology of the blebs, frozen samples were cut with an ion beam to expose a cross-section of a bleb. Figure 3C shows the bleb before cutting, while Figure 3D shows the same bleb after cutting. Though the image is not perfectly clear, it seems to present a hollow center of the bleb, supporting our supposition that the vesicles have open lumens.

3.3. Characterization of Bleb Morphology and Mechanical Resilience by AFM. Blebs were further characterized by AFM imaging and force spectroscopy. A typical image of an individual bleb, formed using 0.01% FA, is shown in Figure 4A. Following imaging, force indentation curves were obtained on individual blebs at their highest point. Due to spontaneous rupturing of a dilute number of vesicles necessary for imaging, a relatively small number of force plots were collected. Figure 4 summarizes the breakthrough force data that were collected. The breakthrough force is defined as the force required for the tip to break through the bilayer, as shown in a typical plot in Figure 4B for 0.01% FA generated blebs and depicted in the cartoon inset. In can be seen in Figure 4C that the 4% FA blebs are significantly more resilient than the 0.01% FA or 0.075% blebs, as the mean force required to break 4% FA blebs is about three times higher. Serum-starvation-generated blebs are even more resilient, almost four times higher.

It is also worth pointing out that blebs form in a range of sizes, some being smaller than 150−200 nm, as seen in the SEM images in Figure 3. In the AFM image in Figure 4A, the bleb has a height of ∼25 nm, lower than might be expected from the NTA and SEM data, but we believe it is somewhat flattened due to its affinity for the underlying surface (a cationic PLL coating to promote sticking during these experiments). We note that upon indentation, in some blebs, two penetration events of the two bilayers are observed. In other cases, as in Figure 4B, both bilayers are compressed and the tip penetrates both at once, as can be seen from the break event spanning ∼10 nm, from ca. 15 to ca. 5 nm.

Care should be taken when comparing data of break-force values as the break force depends on the diameter of the indenting tip, its spring constant, approach speed of the tip, the buffer conditions, the exact lipid composition, temperature, and phase state of the bilayers.[45] Our values are, however, well in line with previously published data from similar studies where bilayer breakthrough forces are reported.[46,47]

These results importantly demonstrate that blebbing conditions have an impact on the resilience of blebs and therefore may directly affect rupture efficiency. Differences in rupture efficiency may, in turn, lead to differences in observed protein mobility, which we examine later. It is therefore important to select the optimal blebbing conditions, which would allow efficient rupture of blebs and sufficient protein mobility.

3.4. Cell Membrane Bleb Bilayer formation. Cell membrane blebs generally do not rupture to form the contiguous, planar bilayer on glass by themselves. Therefore, fusogenic lipid vesicles are used to facilitate rupture of cell blebs and healing together of isolated bilayer patches. Harvested cell blebs were added into PDMS wells and incubated on the glass surface directly. After incubation, POPC liposomes were added into the PDMS well to commence planar bilayer formation and healing (Figure 1). In previous work,[16] the mechanism of formation of planar bleb bilayer was verified by quartz crystal microbalance with dissipation measurements and direct

DOI: 10.1021/acsami.7b07500
ACS Appl. Mater. Interfaces XXXX, XXX, XXX−XXX

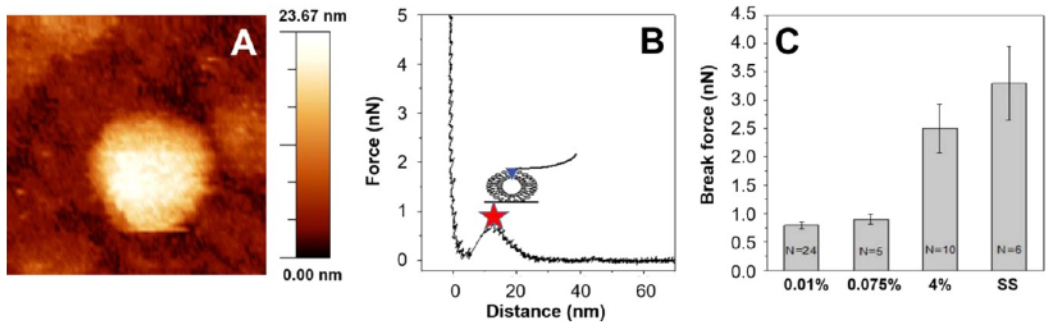

Figure 4. (A) Typical images of an adsorbed bleb (0.01% FA) on a PLL surface prior to indentation. (B) Typical force−distance curve obtained on a 0.01% FA bleb. Cartoon inset shows a schematic depiction of the breakthrough event. Asterisk marks the location of the break event. (C) Breakthrough forces of blebs at four different blebbing conditions, 0.01%, 0.075%, 0.4% FA, and serum-starved (SS).

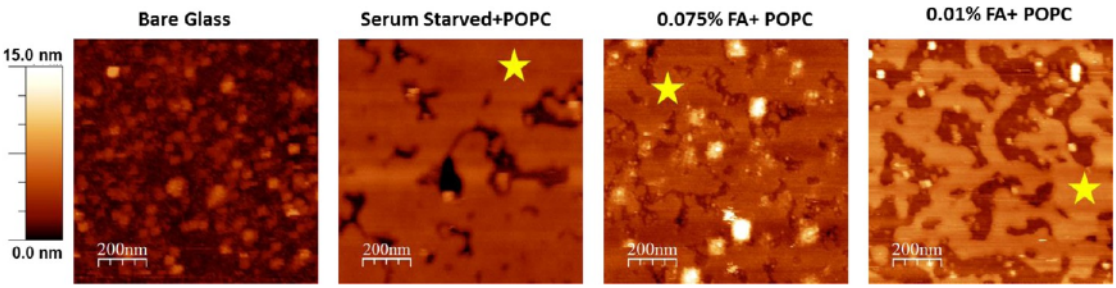

Figure 5. AFM images of bleb bilayers formed after addition of POPC vesicles and bare glass control. Areas chosen for these images were intentionally picked with defects, so that the difference between bare glass and the bilayer surface could be gleaned from the image to assess bilayer formation. Areas covered by bilayers are marked with yellow stars.

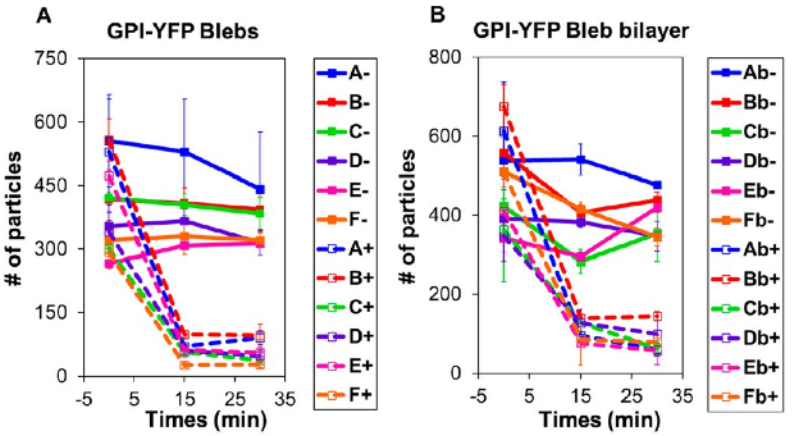

Figure 6. Protease cleavage assay for GPI-YFP orientation. (A) GPI-YFP protein orientation in the cell blebs. At $t = 0$, proteinase K was added to the blebs and cleaved all accessible proteins. Signal drops indicate the GPI-YFP was accessible to the protease. (B) Bleb bilayer was treated using an identical procedure as blebs, and a similar trend indicates the protein has the same orientation in cell blebs and cell bleb bilayers as in the cell plasma membrane.

observation of membrane-bound fluorescent species diffusing from ruptured blebs.

In this set of experiments, we aim to demonstrate the formation of bilayers by AFM. We examined bilayers created from the various blebbing conditions, aided by the addition of POPC vesicles to rupture blebs into planar patches. Uniform layers with few holes are observed in all cases, occasionally with overlying nonruptured blebs. For all bleb types, we observe that the addition of POPC vesicles facilitates the formation of planar bilayers. Bilayers with holes are shown intentionally in Figure 5 to contrast the bilayer with the underlying substrate. We note that smooth-hole-free bilayers can be formed readily, which

DOI: 10.1021/acsami.7b07500
ACS Appl. Mater. Interfaces XXXX, XXX, XXX−XXX

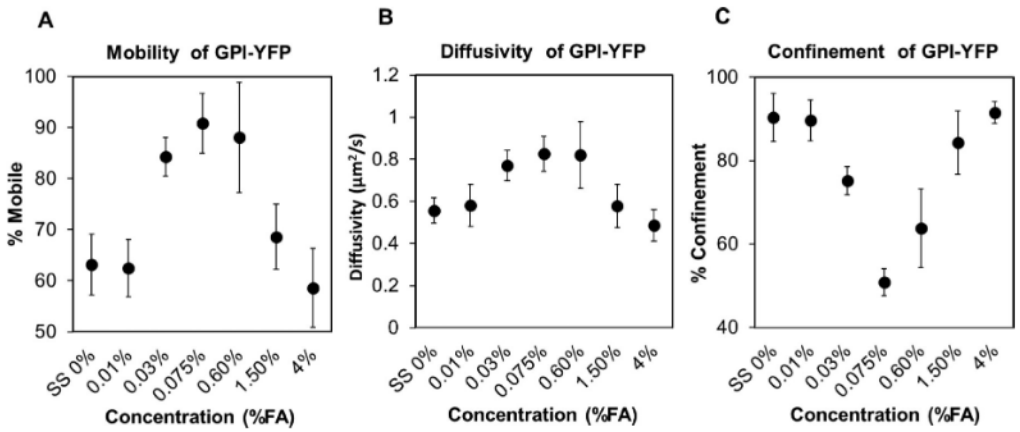

Figure 7. Single-molecule tracking for the motion of individual GPI-YFP protein. (A) Mobility of GPI-YFP in bleb bilayer formed by different kind of cell blebs. (B) Diffusivity of GPI-YFP in bleb bilayer. (C) Confinement of GPI-YFP in bleb bilayer.

look exactly like the bilayer patches denoted by the yellow stars in each image covering the entire field of view.

Although this analysis and previous studies using quartz crystal microbalance and imaging verify the formation of planar bleb bilayers, to use the planar bleb bilayer as biomimetic platform requires protein orientation to be the same as native mammalian cells. In the next sections, we present our results on investigations of the impact of various blebbing conditions on protein and lipid orientation in both cell blebs and bleb bilayers.

3.5. Characterization of GPI-YFP Protein Orientation in Blebs and Planar Bilayers. Important features of mammalian cell blebs are their abilities to be transformed into supported planar bilayers that mimic many features of cell membranes, including their composition and protein content. Hence, understanding the impact of FA/DTT exposure or serum starving on the protein orientation in cell blebs and bleb bilayer is paramount for creating a useful biomimetic material. In order to verify the protein orientation, GPI-YFP plasmid was transfected into the BHK cells and followed by various bleb-inducing treatments. We expect that the orientation of GPI-YFP in blebs is the same as GPI-YFP in the cell membrane because blebs arise as outward protrusions of the cell membrane.[48] Here, assessing protein orientation in blebs and bleb bilayers was carried out by a protease assay. GPI-linked protein is a monotopic peripheral protein and can be cleaved by proteinase K in solution if a GPI-linked protein is located and exposed at the outer leaflet of the spherical bleb or on the upper leaflet of bleb bilayer.[49,50] In the assay, TIRF microscopy was used to monitor each YFP signal, and the signals were counted and tracked to establish the signal loss over time. The proteolytic cleavage of any accessible fluorescent domain of the GPI protein results in the loss of fluorescent signal (YFP) in blebs and bleb bilayers when the cleaved portion floats out of the evanescent field generated during TIRF microscopy. As shown in Figure 6A, control cases were the cell blebs without proteinase K treatment, where GPI-YFP signals remain unchanged over time (except for some photobleaching). However, with proteinase K treatment, blebs have prominent drops in GPI-YFP signals. The results indicate that GPI-YFPs are located on the outer leaflet of cell blebs and can be reached by the protease in all blebbing conditions. In Figure 6B, a very similar trend was observed in the planar bilayers made from the blebs, where the YFP signals remain the same in all control cases over time. Moreover, after adding proteinase K, the proteinase K cleaved most of the GPI-YFP in bleb bilayers and signals of GPI-YFP decreased significantly. These results show that in both cell blebs and bleb bilayers the GPI-YFP protein orientation is maintained as in live cells, facing out. The FA/DTT exposure or serum -starving methods do not affect the GPI-YFP protein orientation in both cell blebs and bleb bilayers.

These results imply that blebs rupture as a "parachute", which keeps luminal sides downward facing the substrates when the bilayer forms,[51,52] and that this mechanism seems to be preserved regardless of the concentration of chemical blebbing agent or serum-starvation process used to generate the blebs. The parachuting rupture mechanism allows GPI-YFP in blebs to remain accessible to bulk solution after forming the bleb bilayer. Importantly, we note that although GPI-YFP orientation and the rupture mechanism determined here were shown not to vary for these proteins as blebbing conditions changed, it is possible that this is not the case for every cell line and membrane protein.

3.6. Characterizing the Mobility and Confinement of Individual Membrane Proteins in Planar Bilayers Using Single-Molecule Tracking. After confirming protein orientation in bleb SLBs, protein mobility in them was assessed. Mobile proteins are essential for a biomimetic bilayer, but it is well documented that formaldehyde is a nonspecific cross-linking reagent and dithiothreitol reduces disulfide bonds and palmitoylated cysteines, which can impact phase partitioning.[20−22] The goal here was to assess the impact of these reagents on protein mobility and protein confinement and compare against the case of serum starving. Protein mobility was assessed using single-molecule tracking analysis by TIRF microscopy. For data analysis, a particle confined in an area smaller than the maximum displacement of fluorescent domain was regarded as immobile. Mean squared displacement (MSD) was used to determine the diffusivity of GPI-YFP. Moment scaling spectrum (MSS) analysis was use to reveal the confinement of GPI-YFP and heterogeneity of the plasma membrane.[37,39] The particle is considered as confined if the value of parameter β is less than 0.4. In Figure 7A and 7B, 0.075% FA GPI-YFP bleb bilayer shows maximums in mobility (at 90.9%) and diffusivity (at 0.83 $\mu m^2/s$). Compared to 0.075% FA condition, cells treated with less FA/DTT (serum starving, 0.01% and 0.03% FA) or higher concentrations (0.6%, 1.5%, and 4% FA) exhibited decreased mobility and diffusivity of GPI-YFP in bleb bilayers. In Figure 7C, 0.075% FA GPI-YFP

DOI: 10.1021/acsami.7b07500
ACS Appl. Mater. Interfaces XXXX, XXX, XXX−XXX

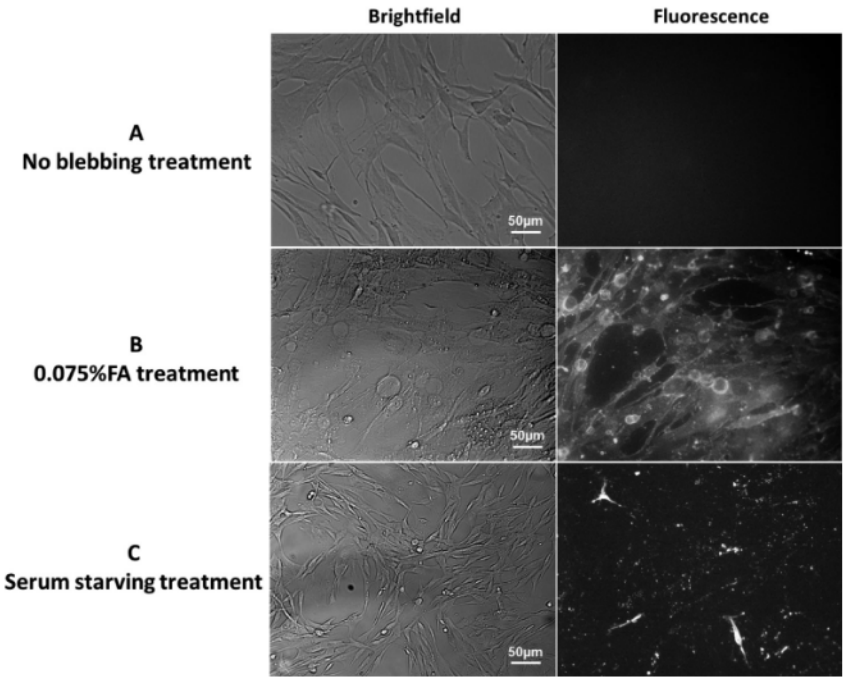

Figure 8. Annexin V assay for determining PS lipid orientation in BHK cells. (A) BHK cells before the blebbing process were treated with annexin V. BHK cells maintain PS asymmetry and show no annexin V binding to the surface of cells. (B) BHK cells after 0.075% FA exposure were treated with the annexin V and show substantial binding of annexin V. (C) BHK cells after the serum starving method were treated with the annexin V and show less annexin V binding overall and more localized binding relative to the chemically induced case.

bleb bilayer also exhibits the least confinement of GPI-YFP. Increasing or reducing FA/DTT from 0.075% FA conditions both leads to the *increase* of confinement of GPI-YFP. The results indicate the 0.075% FA blebbing conditions lead to the maximum mobility and diffusivity of the protein, with minimal protein confinement.

In Figure 7, the diffusivity of GPI-YFP in BHK cell bleb bilayer made from 0.075% FA treatment is reported as 0.83 $\mu m^2/s$. In previous studies,[16] diffusivity of GPI-YFP in bleb bilayers made from 0.075% FA HeLa cell blebs was reported to be around 0.67 $\mu m^2/s$. Diffusivity of GPI-YFP in a cell membrane of a different cell line that we have not examined, COS-7 cells was also analyzed by using various techniques by others and referred to here as a best available point of comparison. The diffusivity of GPI-YFP in COS-7 cell membrane was reported to be 0.73 $\mu m^2/s$ when analyzed by confocal fluorescence recovery after photobleaching[53] and also reported to be 1.2 $\mu m^2/s$ when analyzed by image correlation spectroscopy (ICS) combined with dynamic image correlation spectroscopy (DICS).[54] It is important to note that diffusivity measurements conducted by different techniques and components of the membrane may differ the absolute value, but our results still fall within the reported range of diffusivity of GPI-YFP (0.2−1.3 $\mu m^2/s$).[16,53−57]

There are several possible explanations for the observed trends in protein mobility, diffusivity, and confinement. For the higher FA/DTT concentrations, cross-linking and aggregation of protein may be one rationale for reduced mobility and diffusivity in bleb bilayers. Another plausible explanation is that the blebs are too stiff to rupture, resulting in a significant number of unruptured blebs on the surface. For the lower concentration blebbing agents, the explanation is not as straightforward. One plausible explanation is that the composition of lipid and protein of cell blebs varies as the concentration of chemical-induction condition changes, which is supported to some degree by Western blot analysis (discussed later). For serum starving, these blebs are the most resilient, and so it is reasonable in that case that there would be the most unruptured blebs due to the higher energy required to form the planar structure. In the analysis that follows, more differences between blebs generated by serum starvation and the chemically induced varieties are revealed. It is the changes embodied in this difference that we believe are also reflected in the diffusion results observed here.

3.7. Characterization of Lipid Orientation in Blebs and Bleb Bilayers. To date, lipid orientation in these biomimetic platforms has not been assessed. To investigate the lipid orientation in cell blebs and bleb bilayers, we focused on phosphatidylserine (PS) lipids, as they are known to be asymmetric in the membrane and located on the inner leaflet in live cells and flip to the outer leaflet during early stages of apoptosis.[33] In addition, by using fluorescently labeled annexin V as a marker for PS, we can determine if PS lipids have inverted by binding of annexin V. This annexin V binding assay was used to probe the lipid orientation in blebbed cells, resultant blebs generated from those cells, and bleb bilayers formed from those blebs.

Annexin V was added to cultured BHK cells to determine the PS orientation in cells before and after the blebbing process with serum starving or chemical treatment. Before any treatment with blebbing solutions, the image (Figure 8A) shows that there is no annexin V binding on the surface for BHK cells, that is, the cell plasma membrane maintains PS lipid asymmetry. However, after BHK cells were treated by either serum starving or 0.075% FA/DTT condition, annexin V was observed to bind to the cell surface indicating that PS lipid was now in the externally facing leaflet (Figure 8B and 8C). BHK cells which were treated by the serum-starving method show

DOI: 10.1021/acsami.7b07500
ACS Appl. Mater. Interfaces XXXX, XXX, XXX−XXX

the adhesion of annexin V to PS lipids, but the degree of PS lipid scrambling is apparently much less than the 0.075% formaldehyde-treated condition. Additionally, the binding pattern of the serum-starving case seems to be more localized (punctate), perhaps at sites where blebs were released, supporting that the mechanism of serum-starvation-induced bleb release is different than chemically induced blebs where it is observed that the fluorescence is more diffuse. In the chemically induced case, cells are slowly dying, and so it stands to reason that PS would be flipped to the other leaflet. Serum starving seems to lead to another pathway, such as exocytosis, where cells are not yet dying but shedding materials in response to the deficient media. Nonetheless, both chemical induction and serum starving cause PS lipids to flip to the outer leaflet of BHK cells, albeit to different degrees.

PS lipid orientation in cell blebs and bleb bilayers were characterized by annexin V assay as well. Plain POPC bilayer served as a negative control experiment ,and the image shows the annexin V does not bind to POPC bilayers (Figure 9A). The 2% PS was mixed with 98% POPC, which served as the positive control, and the image shows that annexin V binds readily to a 2% PS lipid bilayer (Figure 9B). Blebs induced from both serum starving and 0.075% formaldehyde exposure were examined for PS lipid orientation in the following way. Cell blebs were adsorbed on the glass slides, and the rest of the exposed glass substrate was blocked from nonspecific adsorption with BSA. Next, annexin V was added to probe the PS lipids orientation in blebs from both blebbing methods. In either the serum-starving or the chemical exposure method, annexin V bound to the cell blebs, which indicates that the cell blebs also lost PS lipid asymmetry during blebbing (Figure 9C and 9E).

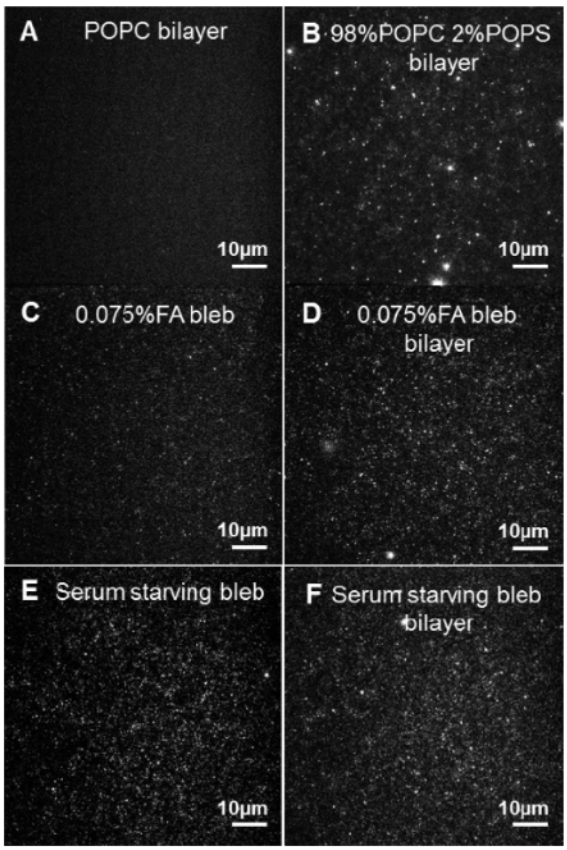

Figure 9. Annexin V assay for PS lipid orientation in cell blebs and bilayer. (A) POPC bilayer and (B) 98% POPC/2% POPS bilayer was used to indicate the annexin V only binds to the PS lipid. Cell blebs from 0.075% FA exposure (C) and serum starving (E) reveal the cell blebs lost PS lipid symmetry. Bleb bilayers made from the cell blebs from 0.075% FA exposure (D) and serum starving (F) indicate the presence of PS lipid facing toward the bulk solution.

Given that cell blebs have already lost PS lipid asymmetry, we anticipated that the bleb bilayers would also lack PS lipid asymmetry. To test this, the annexin V assay was used to quantify bleb bilayer asymmetry. As expected, annexin V bound to the PS lipids in the bleb bilayers also (Figure 9D and 9F).

Apoptosis is a process of programmed cell death. PS externalization on the plasma membrane is the hallmark of apoptosis process.[33] As mentioned above, the blebbing process induced by both serum starving or chemical treatment leads to PS exposure in cells. In some sense this is not a surprising result, as the cells in these culture conditions are not thriving any longer. We also showed that PS is exposed on the outer leaflet in both cell blebs and bleb bilayer, but because the PS is already flipped in the cells, it is not possible to further distinguish by this assay if other lipid types are also flipping during bilayer formation or are already flipped. In the apoptotic situation, the first feature is PS externalization, which leads to phospholipid redistribution and induces apoptotic cell phagocytosis. The second feature is loss of cell volume, which leads to buckling of the membrane and shrinkage of cells, factors necessary for the formation of cell blebs.[58,59] Thus, the apoptosis process and subsequent PS flip are intimately related to the process of generating the cell blebs. We do not know the extent of flip−flop of other lipids at this stage nor if PS flip−flop is a valid universal indicator of loss of all lipid asymmetry in the bilayer. Unfortunately, few other assays are available to test other lipids of known asymmetry at this point in time.

Despite the PS exposure, the cell plasma membrane bleb bilayer importantly preserves the protein orientation and protein activity (described next), making this a beneficial platform for studying membrane protein function and activity and for use in a variety of in vitro applications.

3.8. Characterization of Human Aminopeptidase N Enzyme Activity in Cell Blebs. To evaluate the impact of blebbing conditions on protein activity, an enzymatic assay was performed on cell blebs expressing human aminopeptidase N (hAPN). hAPN is a membrane-bound enzyme, and H-Ala-AMC is the substrate for hAPN.[60] As hAPN cleaves the substrate, the substrate becomes fluorescent. To be consistent across experiments, the concentration of cell blebs was measured by nanoparticle tracking analysis and adjusted to 5×10^8 blebs/mL for each run, diluting and remeasuring concentration by Nanoparticle tracking analysis until the concentration target was reached. The cell blebs were then mixed with 270 mM H-Ala-AMC. Fluorescent signals were monitored and counted continuously by a fluorometer for 1.5 h. Cell blebs devoid of hAPN from the serum-starving method or induced by chemical means were used as negative controls. As shown in Figure 10, the concentration of FA/DTT used during blebbing impacts the activity of hAPN. The blebs induced by 0.01% FA show the highest value of the fluorescence signal, and the blebs induced by 4% FA show the lowest value of the fluorescence signal. The activity of hAPN systematically decreases with increasing concentration of FA/DTT in blebbing solution. Four percent was chosen as the upper limit, as this is the typical amount of formaldehyde used

DOI: 10.1021/acsami.7b07500
ACS Appl. Mater. Interfaces XXXX, XXX, XXX−XXX

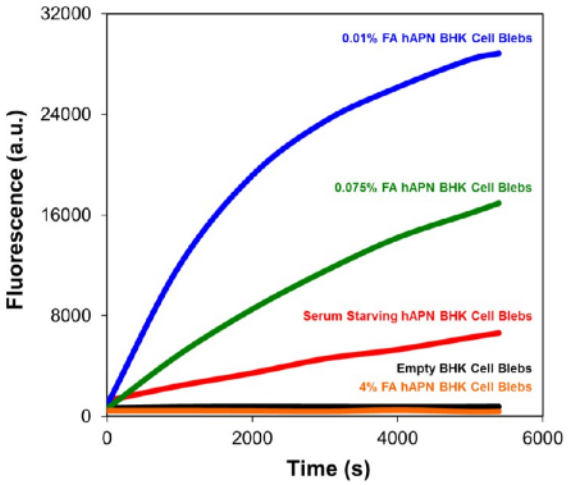

Figure 10. Human aminopeptidase N activity (hAPN) assay. Activity of hAPN in cell blebs from various blebbing conditions was analyzed by enzymatic assay. H-Ala-AMC is the substrate for hAPN. As the hAPN cleaves the H-Ala-AMC, the fluorescent signal releases. Thus, the activity of hAPN is correlated with the intensity of the fluorescent signal.

in cell fixation experiments. Interestingly, at this concentration, activity is almost completely lost but mobility is not, indicating that cross-linking (via formaldehyde) is most likely occurring within the individual proteins (in this case apparently near the substrate binding pocket) rather than between two separate proteins or that DTT has disrupted critical disulfide bonds near the pocket; in either case it is clear the higher the concentration of chemical inductant, the lower the protein activity. Given this trend, it was surprising to us was that the serum-starved blebs were *not* the highest activity.

For the serum-starving case, one plausible explanation for the drop in activity is that the mechanism of bleb formation is different from the chemical treatment and thus proteins may be in different states of maturation or glycosylation when they are blebbed off. Evidence to support that the mechanism of bleb formation differs depending on bleb induction methods coming from the annexin V assay that shows different degrees of annexin V binding in BHK cells after different blebbing solution treatments. However, another possibility for the lower amount of activity is simply that protein content varies with blebbing induction method/conditions, e.g., serum-starved blebs have less enzyme content per concentration of blebs. Thus, we characterize the protein expression level in the next section with Western blots.

3.9. Impact of Blebbing Conditions on hAPN and GPI-YFP Expression. The previous results on hAPN activity suggest that moderate to low FA treatments preserves more protein activity than the serum-starving induction method, which is counter to the expectation that FA can cross-link proteins and DTT reduces disulfide bonds and thus would reduce, not elevate, protein activity. Our initial hypothesis to explain this result was that protein expression levels must be reduced in the serum-starving method relative to the FA/DTT induction method. Thus, to clarify how protein expression levels vary with blebbing treatments, cell blebs from various conditions were used to assess hAPN and GPI-YFP protein expression by Western blot. Cell blebs devoid of hAPN or GPI-YFP from the serum-starving method were also analyzed by Western blot as negative control (N/C). To avoid batch to batch variability, concentrations of the cell blebs were determined by nanoparticle tracking analysis and adjusted to identical concentrations.

In Figure 11A and 11B, Western blots show bands of GPI-YFP (at 50 kDa) and hAPN (at 150 kDa) and cross-linked complexes of GPI-YFP (at 100 kDa) and hAPN (at 300 kDa), which are presumably dimers. We find that this apparent cross-linking of protein only exists in chemical-induced cell blebs and not in serum-starved blebs. This is reasonable as the chemical-

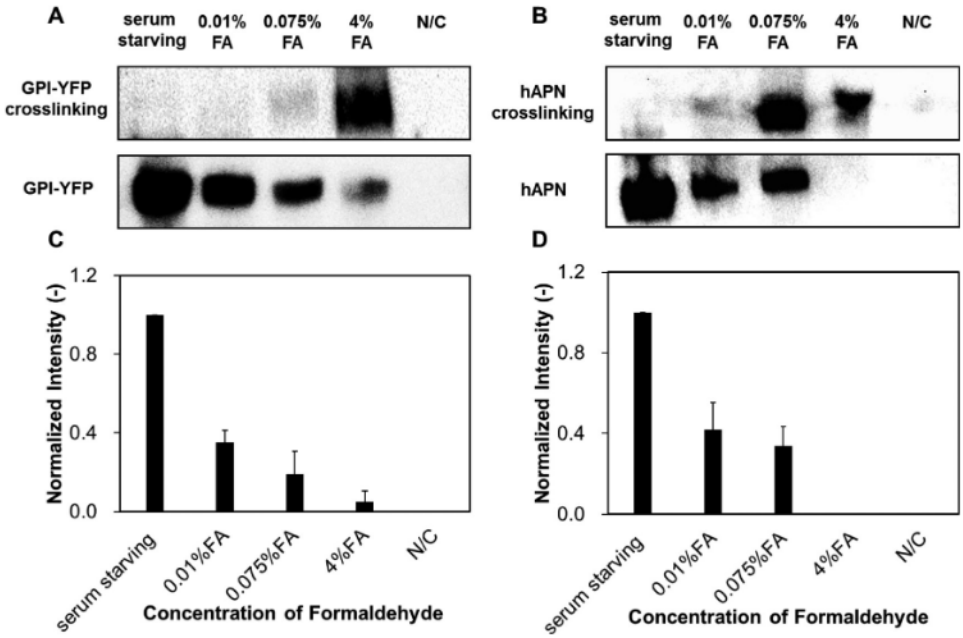

Figure 11. Western blot analysis illustrating the impact of formaldehyde on GPI-YFP and hAPN protein levels. (A) Western blots for GPI-YFP blebs possess the bands of both GPI-YFP and cross-linked complexes. (B) Western blot for hAPN blebs show bands of hAPN and cross-linked complexes. (C) Quantitative analysis of GPI-YFP in Western blot. (D) Quantitative analysis of hAPN in Western blot.

DOI: 10.1021/acsami.7b07500
ACS Appl. Mater. Interfaces XXXX, XXX, XXX−XXX

induction agents used here are known to cause cross-linking and are absent during serum starving. Interestingly, for both proteins, we obtain bands at the known protein molecular weights and twice those weights but nothing higher, and we find that some amount of protein remains in the loading area. We believe this indicates that larger cross-linked protein complexes may not be able to diffuse through the gel. Another possible explanation for the lack of higher weight bands is that the concentration of the bigger cross-linked complexes is too small to detect.

To examine how expression level changes with variation in FA/DTT concentration, bands of GPI-YFP were detected and quantified as FA/DTT increased (Figure 11C). The results show that the protein levels of GPI-YFP decrease with increasing concentration of FA/DTT in the blebbing solution, most likely because of the cross-linking caused by formaldehyde. Interestingly, serum-starved blebs contain the *highest* protein level of GPI-YFP. Similarly, Figure 10D shows that the protein levels of hAPN decrease with increasing concentration of FA/DTT in blebbing solution and that serum starving also yields the *highest* level of hAPN.

In the hAPN enzyme activity assay, the result indicates the activity of hAPN from the serum-starving method is only better than the 4% formaldehyde exposure case, but in the quantitative WB analysis of hAPN, it suggests the serum-starved blebs contain the *highest* protein level of hAPN. This result further supports the hypothesis that the blebbing mechanism is different between serum-starving bleb induction and formaldehyde/DTT exposure. One possibility is that the serum-starving process may trigger the cell to generate not only the cell plasma membrane blebs but also exosomes.[23,61]

From previous literature,[42−44,62] cell plasma membrane blebs and exosomes have distinct origins, but there is still significant controversy in the community over the definitions and properties of the various vesicle types. Exosomes accumulate within multivesicular bodies and are released into the extracellular space during the exocytosis process.[63]Cell plasma membrane blebs, in contrast, bud directly from the cell membrane surface, stimulated by chemical means. Previous literature defines the size of exosomes around 50−100 nm and smaller than cell plasma membrane blebs, which are defined to be around 100−350 nm.[62] Because of the different formation mechanism, these two types of blebs may have different properties such as lipid and protein composition. From our results of size characterization, cell bleb resilience, and protein activity, differences between serum-starving and chemical-induction methods were observed and noted. From our results we make the following observations and interpretations. Blebs generated from serum starving are more resilient, have the most exogenous protein expressed, and exhibit the least exogenous protein activity when compared to blebs generated by moderate chemical-induction methods (that is, excluding the extreme case of 4% FA treatment, which is the typical condition to fix cell surfaces). From our observations we hypothesize that the reason serum-starved blebs have more hAPN protein content but less enzyme activity overall is that these proteins are nonfunctional, or immature, from exosome origin, while fully matured hAPN that has reached the plasma surface is active when it buds off into blebs during chemical induction.

3.10. Implications of This Work. In this study, we characterized cell membrane blebs and bleb bilayers, which reveal the effects of the conditions used to induce blebbing on the protein, lipid, and proteoliposome properties. The results suggest that both induction methods, serum starving or chemical induction, can impact the protein behavior in resulting cell blebs and bleb bilayers. Here we identified conditions that promote proper protein orientation and the best protein fluidity and activity for these materials. The findings provide a well-characterized template for studying protein−lipid, protein−protein, and host−pathogen interactions in a biomimetic system that has many features of cell membranes. Furthermore, the general platform and characterization techniques can be expanded for studying other cell types (e.g., cancer cells, stem cells) with controllable conditions. In other words, these materials can be an advantageous in vitro model for mimicking in vivo cell surface reactions and/or controlling them for the study of phenomena in a variety of applications for biology and pathobiology research.

4. CONCLUSIONS

Planar cell membrane bilayers using cell blebs as an intermediate can be made from several cell lines.[16,21,64] Because of their planar geometry, the bilayer is compatible with a vast array of surface characterization tools. Key advantages of cell bleb bilayers is the ability to create them without the use of detergent or reconstitution while maintaining the richness in composition of the cell membrane itself and the native protein orientation and activity. In this work we characterized cell membrane properties from various blebbing methods/conditions and the impact on protein behavior in them. We show that GPI-YFP has the highest percentage of mobile proteins and least confinement in bilayers created from 0.075% FA/DTT chemical induction. BHK cells exposed to bleb induction conditions display PS lipid externalization when exposed to either serum-starving or chemical-induction methods. Cell blebs and resultant bleb bilayers also lack PS lipid asymmetry. In the hAPN enzyme activity assay, we surprisingly found that cell blebs from 0.01% FA exposure method give the highest enzyme activity, not cell blebs created from serum starving devoid of chemical inducers. However, Western blot analysis shows the cell blebs produced from serum starving express the most protein. From all this analysis we conclude that the blebs that result from these two different induction methods are significantly different in various ways. This conclusion is further supported by characterization of bleb resilience by AFM, which reveals that serum-starved blebs have the highest break force compared to any chemically induced blebs. Taken together, we hypothesize that serum-starved blebs are produced by a different mechanism than the chemically induced blebs. One possibility is that serum starvation generates blebs via an exocytotic pathway, whereas the chemically induced blebs blister off from the plasma membrane. In conclusion, we believe this study clarifies conditions and promotes the usage of planar mammalian membrane platforms for emerging research topics like virus−host interactions or interactions between oncogenic microvesicles and cell surfaces.

■ AUTHOR INFORMATION

Corresponding Author

*E-mail: sd386@cornell.edu.

ORCID

Han-Yuan Liu: 0000-0002-9398-6969
Raya Sorkin: 0000-0001-9006-5411
Susan Daniel: 0000-0001-7773-0835

DOI: 10.1021/acsami.7b07500
ACS Appl. Mater. Interfaces XXXX, XXX, XXX−XXX

Notes

The authors declare no competing financial interest.

■ ACKNOWLEDGMENTS

The authors thank Barbara Baird and David Holowka of Cornell University for providing the pYFP-GPI-N1 plasmid and Kathryn Holmes of the University of Colorado for providing the pCI-neo-hAPN plasmid. This work was supported in part by the following grants to S.D.: National Science Foundation (CAREER grant CBET-1149452; CBET-1263701); Memorial Sloan Kettering Cancer Center U54CA199081 subaward BD520101. H.G. was supported in part by a NSF Research Experience for Undergraduates (subaward of CBET-1263701). R.S. acknowledges support through HFSP postdoctoral fellowship LT000419/2015. This work made use of the Cornell Center for Materials Research Shared Facilities supported through the NSF MRSEC program (DMR-1120296). Additional support for the FIB/SEM cryo-stage and transfer system was provided by the Kavli Institute at Cornell and the Energy Materials Center at Cornell, DOE EFRC BES (DE-SC0001086).

■ REFERENCES

(1) Simons, K.; Toomre, D. Lipid Rafts and Signal Transduction. *Nat. Rev. Mol. Cell Biol.* **2000**, *1* (1), 31−39.

(2) Qi, S.; Groves, J. T.; Chakraborty, A. K. Synaptic Pattern Formation During Cellular Recognition. *Proc. Natl. Acad. Sci. U. S. A.* **2001**, *98* (12), 6548−6553.

(3) Kholodenko, B. N. Cell-Signalling Dynamics in Time and Space. *Nat. Rev. Mol. Cell Biol.* **2006**, *7* (3), 165−176.

(4) Gamper, N.; Shapiro, M. S. Regulation of Ion Transport Proteins by Membrane Phosphoinositides. *Nat. Rev. Neurosci.* **2007**, *8* (12), 921−934.

(5) Lingwood, D.; Simons, K. Lipid Rafts as a Membrane-Organizing Principle. *Science* **2010**, *327* (5961), 46−50.

(6) Lee, A. G. How Lipids Affect the Activities of Integral Membrane Proteins. *Biochim. Biophys. Acta, Biomembr.* **2004**, *1666* (1), 62−87.

(7) Seddon, A. M.; Curnow, P.; Booth, P. J. Membrane Proteins, Lipids and Detergents: Not Just a Soap Opera. *Biochim. Biophys. Acta, Biomembr.* **2004**, *1666* (1), 105−117.

(8) Helenius, A.; Simons, K. Solubilization of Membranes by Detergents. *Biochim. Biophys. Acta, Rev. Biomembr.* **1975**, *415* (1), 29−79.

(9) Richter, R. P.; Bérat, R.; Brisson, A. R. Formation of Solid-Supported Lipid Bilayers: An Integrated View. *Langmuir* **2006**, *22* (8), 3497−3505.

(10) Tabaei, S. R.; Choi, J.-H.; Haw Zan, G.; Zhdanov, V. P.; Cho, N.-J. Solvent-Assisted Lipid Bilayer Formation on Silicon Dioxide and Gold. *Langmuir* **2014**, *30* (34), 10363−10373.

(11) Tamm, L. K.; McConnell, H. M. Supported Phospholipid Bilayers. *Biophys. J.* **1985**, *47* (1), 105−113.

(12) Watts, T. H.; Gaub, H. E.; McConnell, H. M. T-Cell-Mediated Association of Peptide Antigen and Major Histocompatibility Complex Protein Detected by Energy Transfer in an Evanescent Wave-Field. *Nature* **1986**, *320* (6058), 179−181.

(13) Chiantia, S.; Ries, J.; Kahya, N.; Schwille, P. Combined Afm and Two-Focus Sfcs Study of Raft-Exhibiting Model Membranes. *ChemPhysChem* **2006**, *7* (11), 2409−2418.

(14) Cho, N.-J.; Frank, C. W.; Kasemo, B.; Höök, F. Quartz Crystal Microbalance with Dissipation Monitoring of Supported Lipid Bilayers on Various Substrates. *Nat. Protoc.* **2010**, *5* (6), 1096−1106.

(15) Terrettaz, S.; Stora, T.; Duschl, C.; Vogel, H. Protein Binding to Supported Lipid Membranes: Investigation of the Cholera Toxin-Ganglioside Interaction by Simultaneous Impedance Spectroscopy and Surface Plasmon Resonance. *Langmuir* **1993**, *9* (5), 1361−1369.

(16) Richards, M. J.; Hsia, C.-Y.; Singh, R. R.; Haider, H.; Kumpf, J.; Kawate, T.; Daniel, S. Membrane Protein Mobility and Orientation Preserved in Supported Bilayers Created Directly from Cell Plasma Membrane Blebs. *Langmuir* **2016**, *32* (12), 2963−2974.

(17) Costello, D. A.; Millet, J. K.; Hsia, C.-Y.; Whittaker, G. R.; Daniel, S. Single Particle Assay of Coronavirus Membrane Fusion with Proteinaceous Receptor-Embedded Supported Bilayers. *Biomaterials* **2013**, *34* (32), 7895−7904.

(18) Costello, D. A.; Hsia, C.-Y.; Millet, J. K.; Porri, T.; Daniel, S. Membrane Fusion-Competent Virus-Like Proteoliposomes and Proteinaceous Supported Bilayers Made Directly from Cell Plasma Membranes. *Langmuir* **2013**, *29* (21), 6409−6419.

(19) Hopwood, D. A Comparison of the Crosslinking Abilities of Glutaraldehyde, Formaldehyde and A-Hydroxyadipaldehyde with Bovine Serum Albumin and Casein. *Histochem. Cell Biol.* **1969**, *17* (2), 151−161.

(20) Fraenkel-Conrat, H.; Olcott, H. S. The Reaction of Formaldehyde with Proteins. V. Cross-Linking between Amino and Primary Amide or Guanidyl Groups. *J. Am. Chem. Soc.* **1948**, *70* (8), 2673−2684.

(21) Sezgin, E.; Kaiser, H.-J.; Baumgart, T.; Schwille, P.; Simons, K.; Levental, I. Elucidating Membrane Structure and Protein Behavior Using Giant Plasma Membrane Vesicles. *Nat. Protoc.* **2012**, *7* (6), 1042−1051.

(22) Levental, I.; Lingwood, D.; Grzybek, M.; Coskun, Ü.; Simons, K. Palmitoylation Regulates Raft Affinity for the Majority of Integral Raft Proteins. *Proc. Natl. Acad. Sci. U. S. A.* **2010**, *107* (51), 22050−22054.

(23) Evdokimovskaya, Y.; Skarga, Y.; Vrublevskaya, V.; Morenkov, O. Secretion of the Heat Shock Proteins Hsp70 and Hsc70 by Baby Hamster Kidney (Bhk-21) Cells. *Cell Biol. Int.* **2010**, *34* (10), 985−990.

(24) Paulick, M. G.; Bertozzi, C. R. The Glycosylphosphatidylinositol Anchor: A Complex Membrane-Anchoring Structure for Proteins†. *Biochemistry* **2008**, *47* (27), 6991−7000.

(25) Nosjean, O.; Briolay, A.; Roux, B. Mammalian Gpi Proteins: Sorting, Membrane Residence and Functions. *Biochim. Biophys. Acta, Rev. Biomembr.* **1997**, *1331* (2), 153−186.

(26) Wulfaenger, J.; Niedling, S.; Riemann, D.; Seliger, B. Aminopeptidase N (Apn)/Cd13-Dependent Cxcr4 Downregulation Is Associated with Diminished Cell Migration, Proliferation and Invasion. *Mol. Membr. Biol.* **2008**, *25* (1), 72−82.

(27) Ashmun, R. A.; Look, A. T. Metalloprotease Activity of Cd13/Aminopeptidase N on the Surface of Human Myeloid Cells. *Blood* **1990**, *75* (2), 462−469.

(28) Yeager, C. L.; Ashmun, R. A.; Williams, R. K.; Cardellichio, C. B.; Shapiro, L. H.; Look, A. T.; Holmes, K. V. Human Aminopeptidase N Is a Receptor for Human Coronavirus 229e. *Nature* **1992**, *357* (6377), 420.

(29) Wurm, F. M. Production of Recombinant Protein Therapeutics in Cultivated Mammalian Cells. *Nat. Biotechnol.* **2004**, *22* (11), 1393−1398.

(30) Drexler, I.; Heller, K.; Wahren, B.; Erfle, V.; Sutter, G. Highly Attenuated Modified Vaccinia Virus Ankara Replicates in Baby Hamster Kidney Cells, a Potential Host for Virus Propagation, but Not in Various Human Transformed and Primary Cells. *J. Gen. Virol.* **1998**, *79* (2), 347−352.

(31) Zhu, J. Mammalian Cell Protein Expression for Biopharmaceutical Production. *Biotechnol. Adv.* **2012**, *30* (5), 1158−1170.

(32) Horcas, I.; Fernández, R.; Gomez-Rodriguez, J.; Colchero, J.; Gómez-Herrero, J.; Baro, A. Wsxm: A Software for Scanning Probe Microscopy and a Tool for Nanotechnology. *Rev. Sci. Instrum.* **2007**, *78* (1), 013705.

(33) Vermes, I.; Haanen, C.; Steffens-Nakken, H.; Reutellingsperger, C. A Novel Assay for Apoptosis Flow Cytometric Detection of Phosphatidylserine Expression on Early Apoptotic Cells Using Fluorescein Labelled Annexin V. *J. Immunol. Methods* **1995**, *184* (1), 39−51.

(34) Vrljic, M.; Nishimura, S. Y.; Moerner, W. Single-Molecule Tracking. *Methods Mol. Biol.* **2007**, *398*, 193−219.

DOI: 10.1021/acsami.7b07500
ACS Appl. Mater. Interfaces XXXX, XXX, XXX−XXX

(35) Sonnleitner, A.; Schütz, G.; Schmidt, T. Free Brownian Motion of Individual Lipid Molecules in Biomembranes. *Biophys. J.* **1999**, *77* (5), 2638−2642.
(36) Poudel, K. R.; Jones, J. P.; Brozik, J. A. A Guide to Tracking Single Transmembrane Proteins in Supported Lipid Bilayers. *Methods Mol. Biol.* **2013**, *974*, 233−252.
(37) Ferrari, R.; Manfroi, A.; Young, W. Strongly and Weakly Self-Similar Diffusion. *Phys. D* **2001**, *154* (1), 111−137.
(38) Smith, M. B.; Karatekin, E.; Gohlke, A.; Mizuno, H.; Watanabe, N.; Vavylonis, D. Interactive, Computer-Assisted Tracking of Speckle Trajectories in Fluorescence Microscopy: Application to Actin Polymerization and Membrane Fusion. *Biophys. J.* **2011**, *101* (7), 1794−1804.
(39) Sbalzarini, I. F.; Koumoutsakos, P. Feature Point Tracking and Trajectory Analysis for Video Imaging in Cell Biology. *J. Struct. Biol.* **2005**, *151* (2), 182−195.
(40) Smith, P. R.; Morrison, I. E.; Wilson, K. M.; Fernandez, N.; Cherry, R. J. Anomalous Diffusion of Major Histocompatibility Complex Class I Molecules on Hela Cells Determined by Single Particle Tracking. *Biophys. J.* **1999**, *76* (6), 3331−3344.
(41) Kusumi, A.; Sako, Y.; Yamamoto, M. Confined Lateral Diffusion of Membrane Receptors as Studied by Single Particle Tracking (Nanovid Microscopy). Effects of Calcium-Induced Differentiation in Cultured Epithelial Cells. *Biophys. J.* **1993**, *65* (5), 2021−2040.
(42) Théry, C.; Ostrowski, M.; Segura, E. Membrane Vesicles as Conveyors of Immune Responses. *Nat. Rev. Immunol.* **2009**, *9* (8), 581−593.
(43) Lee, Y.; El Andaloussi, S.; Wood, M. J. Exosomes and Microvesicles: Extracellular Vesicles for Genetic Information Transfer and Gene Therapy. *Hum. Mol. Genet.* **2012**, *21* (R1), R125−R134.
(44) György, B.; Szabó, T. G.; Pásztói, M.; Pál, Z.; Misják, P.; Aradi, B.; László, V.; Pállinger, É.; Pap, E.; Kittel, Á. Membrane Vesicles, Current State-of-the-Art: Emerging Role of Extracellular Vesicles. *Cell. Mol. Life Sci.* **2011**, *68* (16), 2667−2688.
(45) Garcia-Manyes, S.; Sanz, F. Nanomechanics of Lipid Bilayers by Force Spectroscopy with Afm: A Perspective. *Biochim. Biophys. Acta, Biomembr.* **2010**, *1798* (4), 741−749.
(46) Li, J. K.; Sullan, R. M. A.; Zou, S. Atomic Force Microscopy Force Mapping in the Study of Supported Lipid Bilayers. *Langmuir* **2011**, *27* (4), 1308−1313.
(47) Sullan, R. M. A.; Li, J. K.; Hao, C.; Walker, G. C.; Zou, S. Cholesterol-Dependent Nanomechanical Stability of Phase-Segregated Multicomponent Lipid Bilayers. *Biophys. J.* **2010**, *99* (2), 507−516.
(48) Dogterom, M.; Koenderink, G. Cell-Membrane Mechanics: Vesicles in and Tubes Out. *Nat. Mater.* **2011**, *10* (8), 561−562.
(49) Wu, C. C.; MacCoss, M. J.; Howell, K. E.; Yates, J. R. A Method for the Comprehensive Proteomic Analysis of Membrane Proteins. *Nat. Biotechnol.* **2003**, *21* (5), 532−538.
(50) Fischer, F.; Poetsch, A. Protein Cleavage Strategies for an Improved Analysis of the Membrane Proteome. *Proteome Sci.* **2006**, *4* (1), 2.
(51) Hsia, C.-Y.; Chen, L.; Singh, R. R.; DeLisa, M. P.; Daniel, S., A Molecularly Complete Planar Bacterial Outer Membrane Platform. *Sci. Rep.* **2016**, *6*.10.1038/srep32715
(52) Fuhrmans, M.; Muller, M. Mechanisms of Vesicle Spreading on Surfaces: Coarse-Grained Simulations. *Langmuir* **2013**, *29* (13), 4335−4349.
(53) Kang, M.; Day, C. A.; Kenworthy, A. K.; DiBenedetto, E. Simplified Equation to Extract Diffusion Coefficients from Confocal Frap Data. *Traffic* **2012**, *13* (12), 1589−1600.
(54) Nohe, A.; Keating, E.; Fivaz, M.; van der Goot, F. G.; Petersen, N. O. Dynamics of Gpi-Anchored Proteins on the Surface of Living Cells. *Nanomedicine* **2006**, *2* (1), 1−7.
(55) Kenworthy, A. K.; Nichols, B. J.; Remmert, C. L.; Hendrix, G. M.; Kumar, M.; Zimmerberg, J.; Lippincott-Schwartz, J. Dynamics of Putative Raft-Associated Proteins at the Cell Surface. *J. Cell Biol.* **2004**, *165* (5), 735−746.
(56) Day, C. A.; Kenworthy, A. K. Mechanisms Underlying the Confined Diffusion of Cholera Toxin B-Subunit in Intact Cell Membranes. *PLoS One* **2012**, *7* (4), e34923.
(57) Pautot, S.; Lee, H.; Isacoff, E. Y.; Groves, J. T. Neuronal Synapse Interaction Reconstituted between Live Cells and Supported Lipid Bilayers. *Nat. Chem. Biol.* **2005**, *1* (5), 283−289.
(58) Shiratsuchi, A.; Osada, S.; Kanazawa, S.; Nakanishi, Y. Essential Role of Phosphatidylserine Externalization in Apoptosing Cell Phagocytosis by Macrophages. *Biochem. Biophys. Res. Commun.* **1998**, *246* (2), 549−555.
(59) Bortner, C. D.; Cidlowski, J. A. A Necessary Role for Cell Shrinkage in Apoptosis. *Biochem. Pharmacol.* **1998**, *56* (12), 1549−1559.
(60) Joshi, S.; Chen, L.; Winter, M. B.; Lin, Y.-L.; Yang, Y.; Shapovalova, M.; Smith, P. M.; Liu, C.; Li, F.; LeBeau, A. M., The Rational Design of Therapeutic Peptides for Aminopeptidase N Using a Substrate-Based Approach. *Sci. Rep.* **2017**, *7*.10.1038/s41598-017-01542-5
(61) Raposo, G.; Stoorvogel, W. Extracellular Vesicles: Exosomes, Microvesicles, and Friends. *J. Cell Biol.* **2013**, *200* (4), 373−383.
(62) Cocucci, E.; Meldolesi, J. Ectosomes and Exosomes: Shedding the Confusion between Extracellular Vesicles. *Trends Cell Biol.* **2015**, *25* (6), 364−372.
(63) Heijnen, H. F.; Schiel, A. E.; Fijnheer, R.; Geuze, H. J.; Sixma, J. J. Activated Platelets Release Two Types of Membrane Vesicles: Microvesicles by Surface Shedding and Exosomes Derived from Exocytosis of Multivesicular Bodies and Alpha-Granules. *Blood* **1999**, *94* (11), 3791−3799.
(64) Scott, R. E. Plasma Membrane Vesiculation: A New Technique for Isolation of Plasma Membranes. *Science* **1976**, *194* (4266), 743−745.

DOI: 10.1021/acsami.7b07500
ACS Appl. Mater. Interfaces XXXX, XXX, XXX−XXX